ESC European Society of Cardiology

Cardiovascular Research (2020) **116**, 2207–2215
doi:10.1093/cvr/cvaa267

SARS-CoV-2 infects and induces cytotoxic effects in human cardiomyocytes

Denisa Bojkova[1†], Julian U.G. Wagner[2,3†], Mariana Shumliakivska[2†], Galip S. Aslan[2†], Umber Saleem[3,4], Arne Hansen[3,4], Guillermo Luxán[2], Stefan Günther[5,6], Minh Duc Pham[7], Jaya Krishnan[6,7], Patrick N. Harter[8], Utz H. Ermel[9], Achilleas S. Frangakis[9], Hendrik Milting[10], Andreas M. Zeiher[4,6,7], Karin Klingel[11], Jindrich Cinatl[1], Andreas Dendorfer[4,12], Thomas Eschenhagen[3,4], Carsten Tschöpe[3,13], Sandra Ciesek[1,14,15†], and Stefanie Dimmeler[2,3,6*†]

[1]Institute of Medical Virology, University of Frankfurt, Paul-Ehrlich-Str. 40, 60590 Frankfurt, Germany; [2]Institute for Cardiovascular Regeneration, Centre of Molecular Medicine, Goethe University Frankfurt, Theodor Stern Kai 7, 60590 Frankfurt, Germany; [3]German Center for Cardiovascular Research (DZHK), Germany; [4]Department of Experimental Pharmacology and Toxicology, University Medical Center Hamburg-Eppendorf, Martinistraße 52, 20246 Hamburg, Germany; [5]Max Planck Institute Heart and Lung Research, Ludwigstrasse 43, 61231 Bad Nauheim, Germany; [6]Cardiopulmonary Institute (CPI), Frankfurt, Germany; [7]Department of Medicine, Cardiology, Goethe University Hospital, Theodor Stern Kai 7, 60590 Frankfurt, Germany; [8]Neurological Institute (Edinger Institute), University of Frankfurt, Heinrich-Hoffmann Strasse 7, 60528 Frankfurt, Germany; [9]Institute of Biophysics and BMLS, University of Frankfurt, Campus Riedberg, Maxvon-Laue Strasse 15, 60438 Frankfurt, Germany; [10]Heart and Diabetes Center NRW, University Hospital of the Ruhr University Bochum, Clinic for Thoracic and Cardiovascular Surgery, Erich & Hanna Klessmann Institute, Georgstr. 11, 32545 Bad Oeyenhausen, Germany; [11]Cardiopathology, Institute for Pathology and Neuropathology, University Hospital Tuebingen, Liebermeisterstraße 8, 72076 Tuebingen, Germany; [12]Walter-Brendel-Centre of Experimental Medicine, University Hospital, LMU Munich, Marchioninistr. 27, 81377 Munich, Germany; [13]Department of Cardiology, Campus Virchow Klinikum (CVK), Charité, and Berlin Institute of Health (BIH), Berlin Brandenburger Center for Regenerative Therapies (BCRT), University Medicine Berlin, Berlin, Germany; [14]Fraunhofer Institute for Molecular Biology and Applied Ecology (IME), Branch Translational Medicine and Pharmacology, Theodor Stern Kai 7, 60590 Frankfurt, Germany; and [15]German Centre for Infection Research (DZIF), External partner site, Frankfurt, Germany

Received 8 August 2020; revised 26 August 2020; editorial decision 31 August 2020; accepted 9 September 2020; online publish-ahead-of-print 23 September 2020

Time for primary review: 4 days

Aims Coronavirus disease 2019 is caused by severe acute respiratory syndrome coronavirus 2 (SARS-CoV-2) and has emerged as a global pandemic. SARS-CoV-2 infection can lead to elevated markers of cardiac injury associated with higher risk of mortality. It is unclear whether cardiac injury is caused by direct infection of cardiomyocytes or is mainly secondary to lung injury and inflammation. Here, we investigate whether cardiomyocytes are permissive for SARS-CoV-2 infection.

Methods and results Two strains of SARS-CoV-2 infected human induced pluripotent stem cell-derived cardiomyocytes as demonstrated by detection of intracellular double-stranded viral RNA and viral spike glycoprotein expression. Increasing concentrations of viral RNA are detected in supernatants of infected cardiomyocytes, which induced infections in Caco-2 cell lines, documenting productive infections. SARS-CoV-2 infection and induced cytotoxic and proapoptotic effects associated with it abolished cardiomyocyte beating. RNA sequencing confirmed a transcriptional response to viral infection as demonstrated by the up-regulation of genes associated with pathways related to viral response and interferon signalling, apoptosis, and reactive oxygen stress. SARS-CoV-2 infection and cardiotoxicity was confirmed in a 3D cardiosphere tissue model. Importantly, viral spike protein and viral particles were detected in living human heart slices after infection with SARS-CoV-2. Coronavirus particles were further observed in cardiomyocytes of a patient with coronavirus disease 2019. Infection of induced pluripotent stem cell-derived cardiomyocytes was dependent on cathepsins and angiotensin-converting enzyme 2, and was blocked by remdesivir.

Conclusion This study demonstrates that SARS-CoV-2 infects cardiomyocytes *in vitro* in an angiotensin-converting enzyme 2- and cathepsin-dependent manner. SARS-CoV-2 infection of cardiomyocytes is inhibited by the antiviral drug remdesivir.

[†]The first four authors and the last two authors contributed equally to the study.

*Corresponding author. Tel:+49 69 6301 5158; fax: +49 69 6301 83462, E-mail: dimmeler@em.unifrankfurt.de

Graphical Abstract

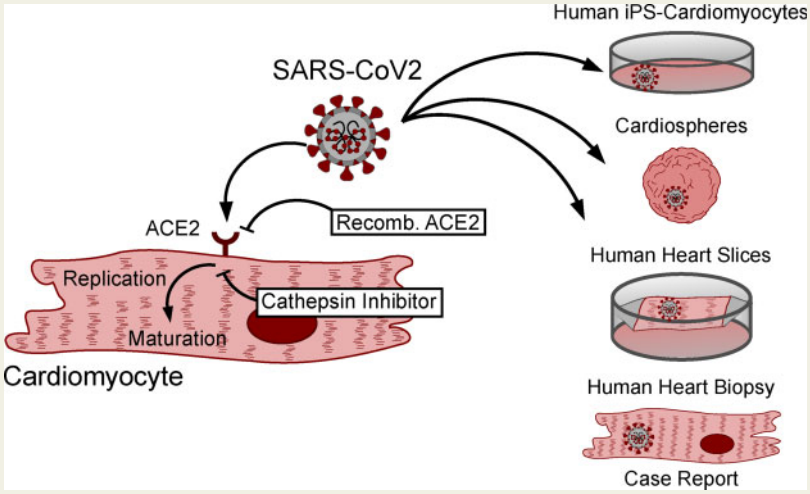

Keywords COVID-19 • SARS-CoV-2 • Cardiomyocyte • Cardiosphere • Heart slice • ACE2

1. Introduction

Coronavirus disease 2019 (COVID-19) is caused by severe acute respiratory syndrome coronavirus 2 (SARS-CoV-2) and has emerged as a global pandemic. SARS-CoV-2 is an enveloped and single-stranded RNA virus type, which mainly invades alveolar epithelial cells and causes adult respiratory distress syndromes. COVID-19 is associated with myocardial injury, as assessed by increased troponin T and N-terminal pro brain natriuretic protein levels accompanying increased cardiovascular symptoms in a significant number of SARS-CoV-2-infected patients.[1–3] Recent studies further demonstrate significantly reduced ejection fraction, higher left ventricular mass, and raised native T1 and T2 assessed by magnetic resonance imaging in patients recovered from severe COVID-19.[4] Elevated levels of cardiac injury markers were associated with higher risk of in-hospital mortality in COVID-19 patients.[5] In patients showing clinical deterioration during COVID-19, left ventricular systolic dysfunction was noted in ~2% of patients according to a very recent study.[6] In addition, patients with underlying cardiovascular disease represent a significant proportion of patients who may suffer from severe courses after COVID-19 infections.[7] However, it is unclear whether elevated biomarkers of cardiac injury and long-term effects on the cardiovascular system are directly caused by viral infection of cardiac tissue or are secondary to hypoxia and systemic inflammation during complicated COVID-19 courses. Earlier studies with cardiac tissue samples revealed mixed results. While one study did not find evidence for viral particles of the first SARS coronavirus SARS-CoV,[8]SARS-CoV RNA was identified in 35% of autopsied human heart samples obtained from patients who succumbed to the SARS crisis during the Toronto SARS outbreak.[9] Other studies suggest that the Middle East respiratory syndrome-related coronavirus, which has similar pathogenicity to SARS-CoV-2, can cause acute myocarditis and heart failure.[10] Moreover, substantial amounts of viral SARS-CoV-2 RNA were detected in human hearts of COVID-19 patients.[11–14] Although virus particles were identified in interstitial cells in myocardium of one patient,[15] direct infection in cardiomyocytes of COVID-19 patients has not yet been described.

Single-cell RNA sequencing and histological analyses demonstrated that human cardiomyocytes express the putative SARS-CoV-2 receptor angiotensin-converting enzyme 2 (ACE2), particularly in patients with cardiovascular diseases,[16,17] suggesting that cardiomyocytes could be targeted by SARS-CoV-2.

Therefore, we investigated whether SARS-CoV-2 infects human-induced pluripotent stem cell-derived cardiomyocytes (hiPS-CMs) in culture and in two models of human cardiac tissue including human heart slices *in vitro*.

2. Methods

The use of all human cells and tissues was approved by the institutional ethics review boards and complies with the Declaration of Helsinki. All subjects gave informed written consent.

2.1 Cell culture

hiPS-CMs of two donors were obtained with an embryoid body-based protocol as described.[18] Cardiospheres were generated by adapting a previously described protocol[19] using hiPS cells. Living human heart slices (300 µm) were generated and cultured as described.[9]

2.2 Viral infection

SARS-CoV-2-FFM1 and -FFM2 were isolated and propagated in Caco-2 cells as described.[20,21] The viral stock was diluted to the desired multiplicity of infection (MOI) in medium containing 1% foetal bovine serum and incubated with cells for 2 h. Then the infectious inoculum was removed and cells were supplemented with the respective culture medium.[18] Cardiospheres were cultured with 25 µL of viral stock [1×10^7 TCID (tissue culture infectious dose) 50/mL] and living human heart slices were incubated with 200 µL of viral stock (1×10^7 TCID50/mL) for 3–5 days.

Quantification of SARS-CoV-2 RNA in cell culture supernatants was performed as previously described.[21] For detection of viral titre, hiPS-CMs were infected for 2 h, the infection medium was replaced, and supernatants were collected 48 h post-infection and used to infect confluent layers of Caco-2 cells in 96-well plates. Cytopathogenic effects were assessed visually 48 h after infection. The infectious titre was determined as TCID50/mL.

For further details, see Supplementary material online, *Expanded Methods*.

3. Results

3.1 Expression of the receptor and co-receptor

We first addressed whether hiPS-CMs showed expression of the SARS-CoV-2 receptor ACE2 and the serine proteases transmembrane protease, serine 2 (TMPRSS2) and cathepsins, which mediate priming of the viral spike protein.[22] ACE2 was well expressed at the mRNA level in hiPS-CMs but not in undifferentiated iPS cells (*Figure 1A* and Supplementary material online, *Figure S1A–D*). Cathepsins B and L were highly expressed, whereas TMPRSS2 was detected only at very low levels by RNA sequencing (*Figure 1A*). Quantitative RT–PCR confirmed the expression of ACE2, but TMPRSS2 was below the detection level (*Figure 1B and C*). ACE2 protein expression was confirmed by immunostaining using two different antibodies in iPS-CMs (*Figure 1D* and Supplementary material online, *Figure S1B and D*). Interestingly, ACE2 expression in cardiomyocytes was lower and ACE2 was localized more to cytoplasmic and perinuclear regions as compared with other TMPRSS2-positive cells such as the human Caco-2 cell line, which is known to be highly permissive for SARS-CoV and SARS-CoV-2 infection [21–23] (*Figure 1B* and Supplementary material online, *Figure S1E*). However, membrane staining was occasionally detected in control and SARS-CoV-2-infected iPS-CMs (Supplementary material online, *Figure S1D and F*; indicated by arrows). These data document that human cardiomyocytes possess receptors and activators described thus far to be necessary for effective SARS-CoV-2 infection, but show a lower expression and distinct localization of ACE2.

3.2 hiPS-CMs are infected by SARS-CoV-2

To test if hiPS-CMs are directly targeted and are permissive for SARS-CoV-2 infection, hiPS-CMs were infected with isolates of SARS-CoV-2[20] (*Figure 2A*). SARS-CoV-2-infected hiPS-CMs showed increased intracellular double-stranded virus RNA as demonstrated by immunostaining (*Figure 2B* and Supplementary material online, *Figure S2A*). Viral RNA in supernatants was further assessed by PCR and was dose and time dependently increased after infection with SARS-CoV-2 (*Figure 2C–E*). Consistently, the expression of the viral spike glycoprotein was detected in a time- and dose-dependent manner after infection with different strains of the virus (FFM1 and FFM2[20]) (*Figure 2F–H* and Supplementary material online, *Figure S2C and D*). Control experiments confirmed spike protein expression in α-sarcomeric actinin-

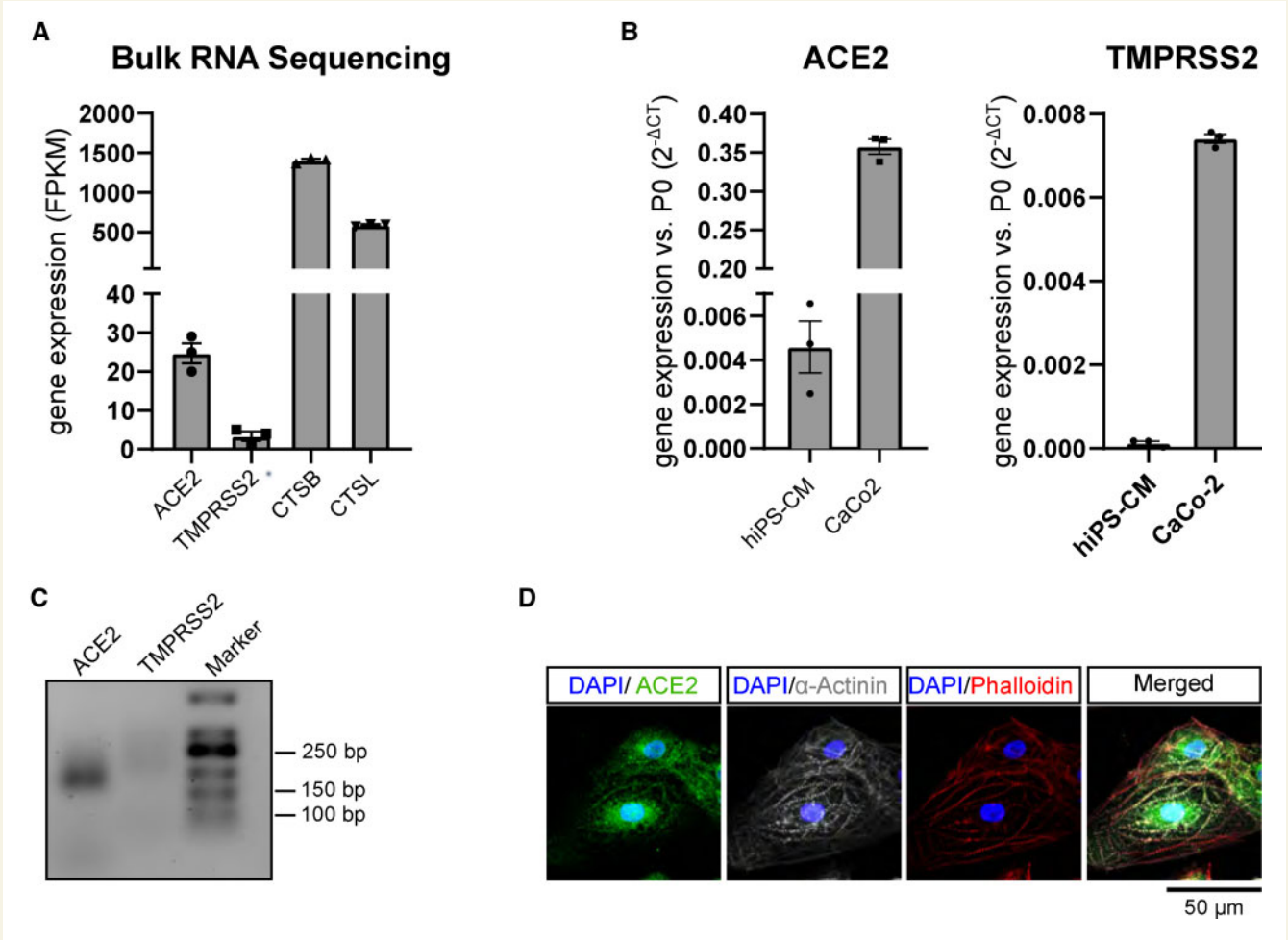

Figure 1 Expression of SARS-CoV-2 receptors and co-activators in hiPS-derived cardiomyocytes. (*A*) Expression in RNA sequencing data of hiPS-CMs ($n = 3$, biological replicates). (*B* and *C*) Confirmation by quantitative RT–PCR ($n = 3$, biological replicates); (*C*) A representative gel. (*D*) ACE2 protein expression was detected by antibody (Abcam) in hiPS-CMs. Cells were counterstained by α-sarcomeric actinin and DAPI. A representative experiment out of six biological replicates of two different iPS-CM donors is shown.

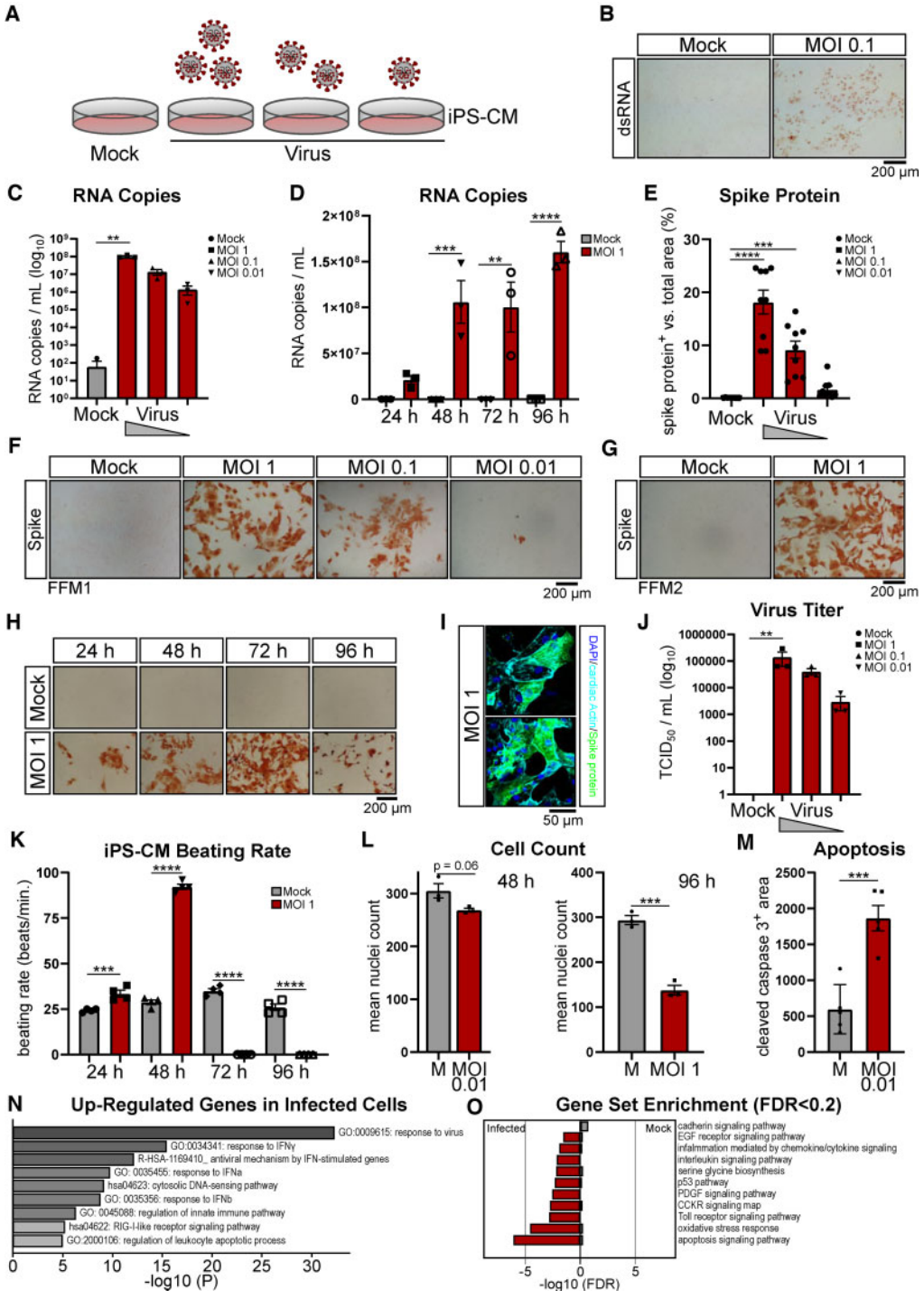

Figure 2 SARS-CoV-2 infects iPS-derived cardiomyocytes. (*A*) Design of the experiment. (*B*) Immunostaining of double-stranded RNA (dsRNA) in hiPS-CMs after infection with SARS-CoV-2 FFM1 for 48 h. (*C* and *D*) SARS-CoV-2 RNA was measured by quantitative RT–PCR in the supernatant of infected hiPS-CMs (*D*, 48 h; *E*, MOI 1). $n = 3$ biological replicates in (*C*) and (*D*). (*E–H*) Spike glycoprotein was measured by immunohistochemistry after infection with isolate SARS-CoV-2 FFM1 (*F*, *H*, and *I*) or SARS-CoV-2 FFM2 (*G*). (*E*) A dose–response curve with $n = 9$ biological replicates. (*I*) Counterstainings with α-sarcomeric actinin confirmed expression of spike protein in hiPS-CMs (48 h). (*J*) Infectious virus in supernatants from infected hiPS-CMs was determined by titration in Caco-2 cells 48 h post-infection. $n = 3$ biological replicates. (*K*) Beating rate of hiPS-CMs. $n = 4$ biological replicates. (*L*) Number of cells (DAPI+ nuclei) after 48 h (MOI 0.01) or 96 h (MOI 1) of infection vs. mock (M) control. $n = 3$ biological replicates. (*M*) Quantification of cleaved caspase-3+ area after 48 h of infection vs. mock (M). $n = 3$ biological replicates. (*N* and *O*) RNA sequencing of mock or SARS-CoV-2-infected hiPS-CM (MOI 1, 48 h), $n = 3$ biological replicates. (*N*) GO term analysis (Metascape) of the top up-regulated genes (>5-fold, FDR <0.2). $n = 3$ biological replicates. (*O*) Top10 enriched terms in the PANTHER database for differentially expressed genes, FDR <0.2. Data are mean±SEM analysed by using two-sided, unpaired *t*-test (*K* and *L*), ordinary one-way ANOVA with *post hoc* Tukey's (*E* and *M*), Dunn's (*F*) comparison, or Kruskal–Wallis test with Dunn's comparison (*D* and *K*). MOI, multiplicity of infection; FDR, false discovery rate. $^{**}P < 0.01$, $^{***}P < 0.001$, $^{****}P < 0.0001$.

expressing cardiomyocytes (*Figure 2I* and Supplementary material online, *Figure S1F*). The supernatant of hiPS-CMs contained fully infectious virus, as demonstrated by titration in Caco-2 cells (*Figure 2J*), indicating that the virus undergoes full replicatory cycles in hiPS-CMs. Interestingly, the frequency of beating was significantly augmented at 24- to 48 h post-infection, but was abolished at later time points (*Figure 2K*). SARS-CoV-2 infection reduced cell counts (*Figure 2L*) and augmented apoptosis in hiPS-CMs (*Figure 2M*). Profound cytopathogenic effects were visible at later time points (96 h) (*Figure 2H*). Cytotoxicity in cardiomyocytes was detected at later time points compared with Caco-2 cells, which quickly round up and showed severe cytotoxicity at 24 h (Supplementary material online, *Figure S2E and F*). RNA sequencing demonstrated that infected hiPS-CMs showed a strong transcriptional response to viral infection including interferon activation (*Figure 2N*) and signatures of apoptosis and oxidative stress (*Figure 2O*).

3.3 SARS-CoV-2 infects cardiomyocytes in 3D cardiac tissue

Next, we determined if SARS-CoV-2 infects cardiomyocytes in a 3D tissue environment using human cardiospheres generated by hiPS cells, which are generated by a modified previously published protocol[19] (*Figure 3A and B*). SARS-CoV-2 time dependently affected beating frequency of cardiospheres, with a profound inhibition at 5 days post-infection (*Figure 3C*). At 5 days post-infection, cardiospheres showed a reduced size (*Figure 3D*) consistent with the induction of cell death. SARS-CoV-2 infection was further documented by spike protein staining (*Figure 3D* and Supplementary material online, *Figure S3*).

Finally, we addressed whether SARS-CoV-2 infects human heart tissue by using living human cardiac tissue slices, which were obtained from explanted hearts[24] (*Figure 4A–F*). Here, increased spike protein expression was shown in four different samples derived from three explants (*Figure 4C–E*). Infection was associated with morphological signs of tissue injury such as areas with loss of α-saromeric actinin signal and disorganized structure compared with homogenous mock controls (*Figure 4C*). Spike protein expression was detected in α-sarcomeric actinin-positive cardiomyocytes (*Figure 4D*). The virus was further identified in infected human heart tissue in cardiomyocytes by electron microscopy (*Figure 4F* and Supplementary material online, *Figure S4*). Of note, stages of the entire replicatory cycle were detected (*Figure 4F*, right panel). Finally, we detected SARS-CoV-2 in an endomyocardial biopsy of a patient with COVID-19. This 27-year-old patient was diagnosed with COVID-19 and suffered a

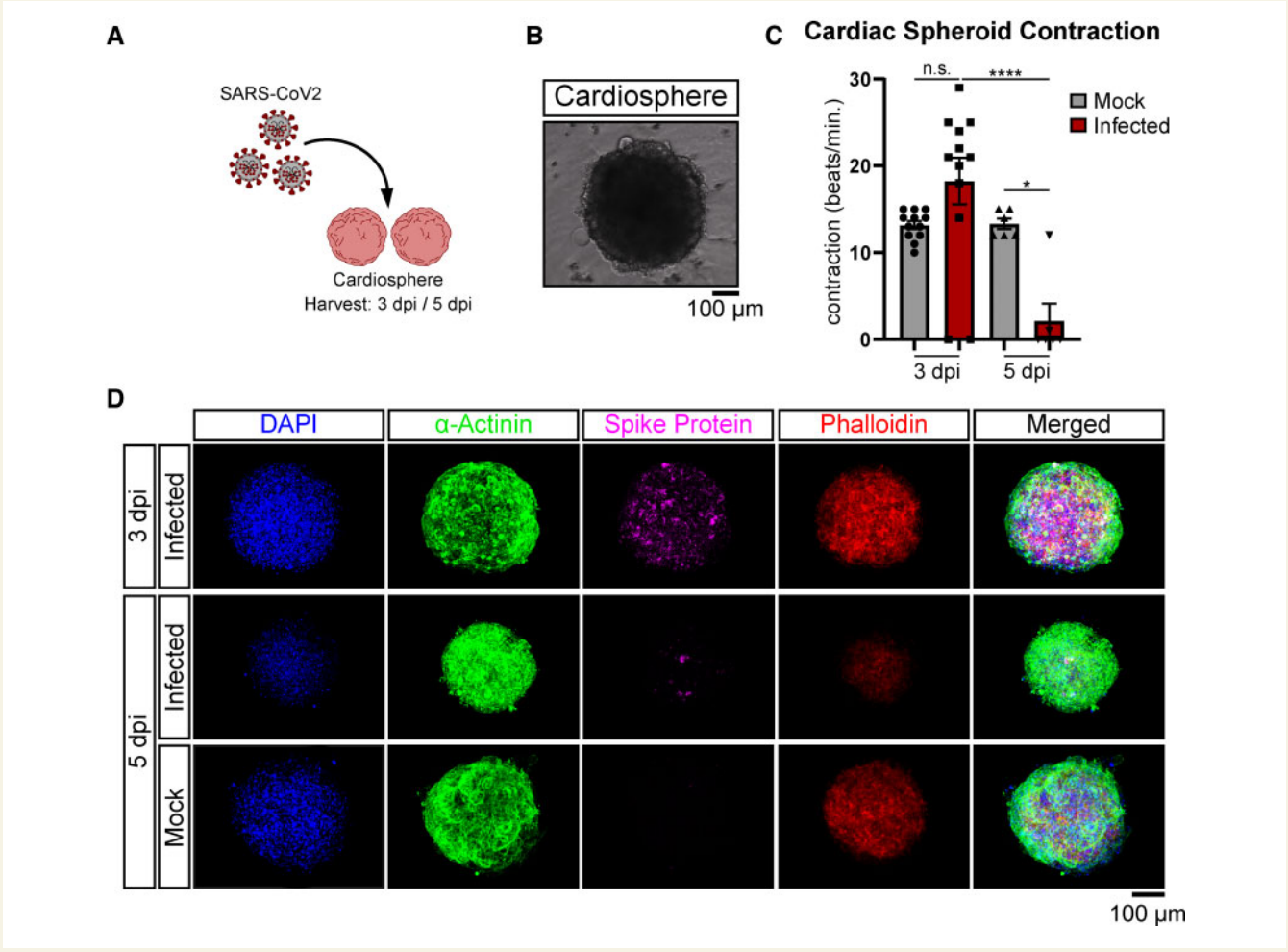

Figure 3 SARS-CoV-2 infects iPS-derived human cardiospheres. (*A*) Study design of cardiosphere infection. (*B*) hiPS-derived cardiosphere (light microscope image). (*C*) Beating frequency of cardiospheres at 3- and 5 days post-infection (dpi). $n = 12$ (3 dpi); $n = 6$ (5 dpi), all biological replicates. (*D*) Expression of spike glycoprotein at 3 and 5 dpi. Data were statistically assessed using one-way ANOVA with *post hoc* Tukey's test. NS, not significant; $^{*}P < 0.05$; $^{****}P < 0.0001$.

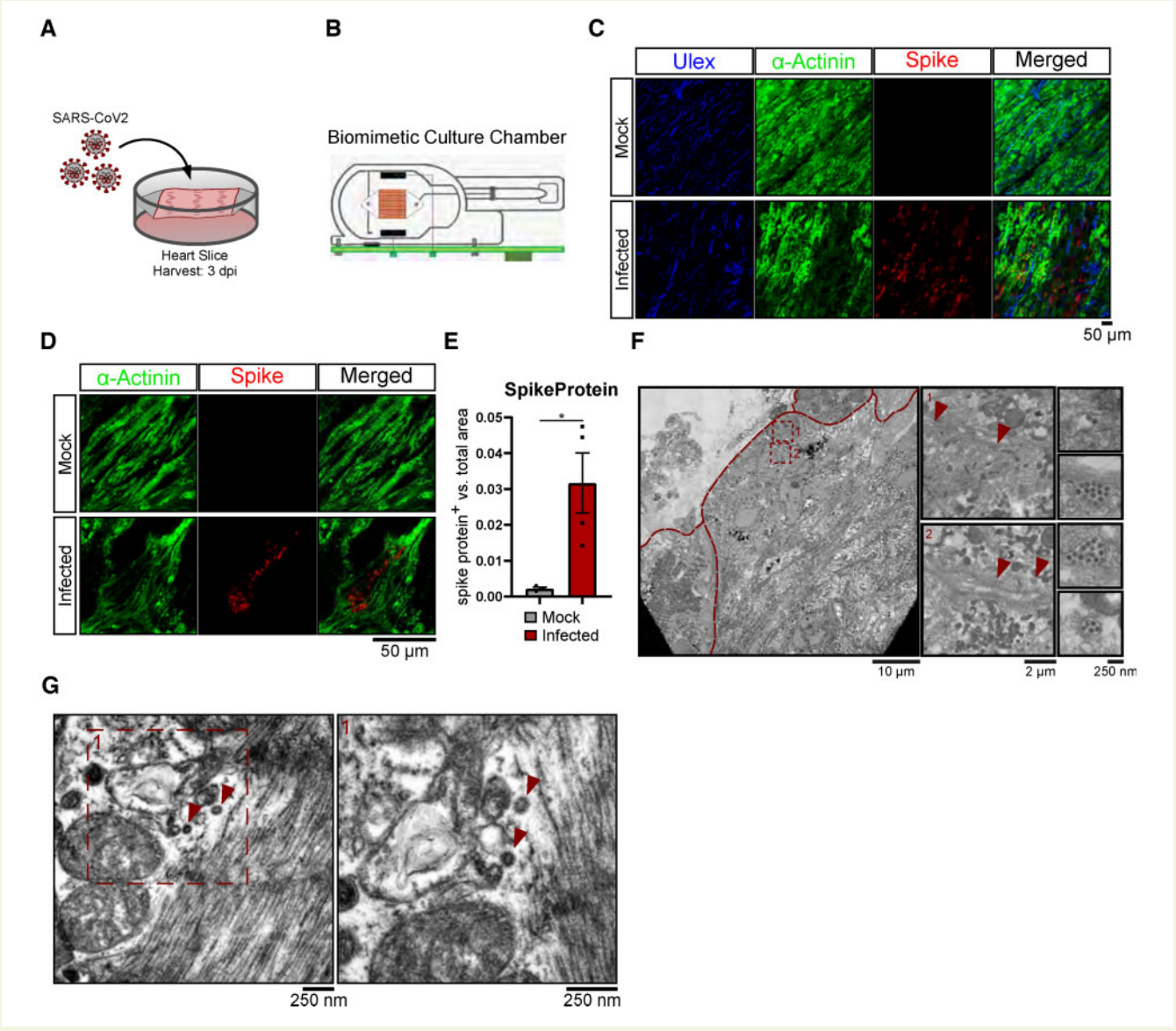

Figure 4 SARS-CoV-2 infects living human cardiac tissue slices. (*A–C*) Infection of human cardiac tissue slices of three explants. (*B*) Scheme of the experiment. (*C–E*) Spike protein expression in infected human heart slices ($n = 4$ samples of three different explants, biological replicates). Quantification of individual images of each explant is shown in (*E*). Data were statistically assessed with unpaired *t*-test with Welch's correction. $^{*}P < 0.05$. Representative images are shown in (*C*), a higher magnification of a representative cardiomyocyte expressing spike protein is shown in (*D*). (*F*) Electron microscopy of infected human cardiac tissue slices. Arrowheads indicate putative virus particles. (*G*) Electron microscopy of a human endomyocardial biopsy taken from a COVID-19 patient. Arrowheads indicate putative virus particles.

complicated course of COVID-19 with severe lung injury and reduced right and left ventricular ejection fraction (see Supplementary material online, *Expanded Methods* for more detail). Virus particles were detected in cardiomyocytes associated with visible cytotoxic effects such as focal loss of myofibrils (*Figure 4G*).

3.4 Cathepsin and RNA-dependent RNA polymerase inhibitors prevent iPS-CM infection

Having demonstrated that SARS-CoV-2 can infect human cardiomyocytes, we tested strategies to interfere with viral infection. First, we determined if interfering with ACE2, which was shown to block virus infection of organoids,[25] is also effective in cardiomyocytes. Indeed, recombinant ACE2 or neutralizing antibodies blocked spike protein expression (*Figure 5A*). Since cardiomyocytes essentially lack TMPRSS2 but express cathepsins, we additionally tested the effect of the protease inhibitor *N*-acetyl-L-leucyl-L-leucyl-L-methionine (ALLM), which preferentially blocks cathepsins.[26] Indeed, inhibition of cathepsins reduced spike protein expression (*Figure 5B*). Moreover, the viral RNA-dependent RNA polymerase inhibitor remdesivir inhibited spike protein expression (*Figure 5C*).

4. Discussion

Altogether, SARS-CoV-2 can infect human cardiomyocytes in culture as well as in two different models of cardiac tissue. Infection was

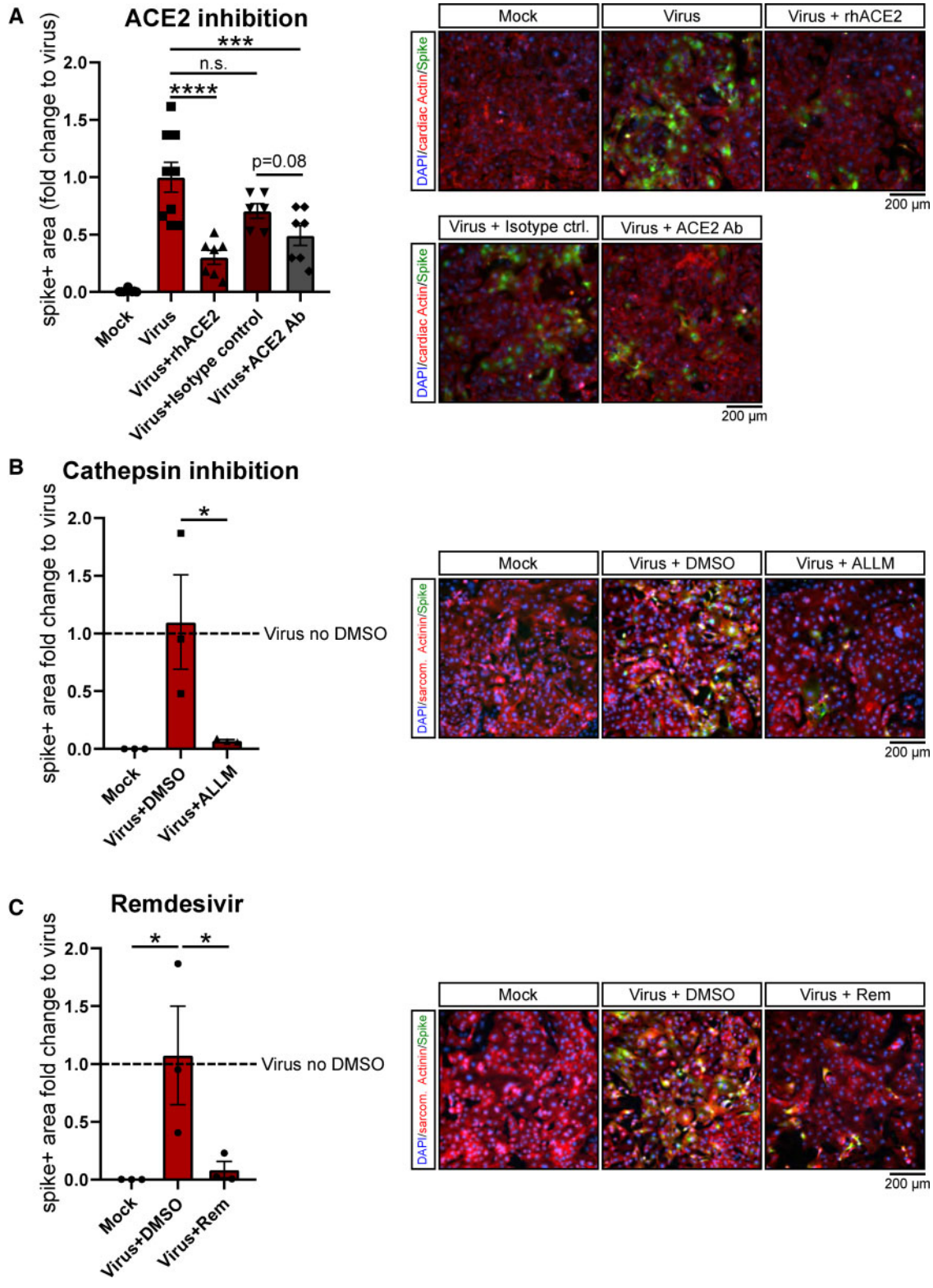

Figure 5 Cardiomyocyte infection is inhibited by ACE2, cathepsin, and RNA polymerase inhibition. (*A*) Effect of recombinant ACE2 (5 µg/mL) or neutralizing antibodies (80 µg/mL) on SARS-CoV-2 infection. Spike protein was quantified after 48 h of infection (MOI=1). $n = 9$ (virus), $n = 7$ (virus+rhACE2), $n = 6$ (isotope control), and $n = 7$ (virus+ACE2 AB), all biological replicates. (B) Effect of the protease inhibitor *N*-acetyl-L-leucyl-L-leucyl-L-methionine (ALLM; 1 µM; added during and post-infection) on spike protein expression after infection with SARS-CoV-2 (MOI=1) at 48 h. $n = 3$ biological replicates. (*C*) Effect of remdesivir (1 µM, added post-infection). Since ALLM and remdesivir were dissolved in DMSO, virus-infected cells were also treated with DMSO in (*B*) and (*C*). $n = 3$ biological replicates. Data were statistically assessed using one-way ANOVA with *post hoc* Dunnett's (*A* and *B*) or *post hoc* Holm–Sidak's test (*C*). NS, not significant; $^{*}P < 0.05$, $^{***}P < 0.001$, $^{****}P < 0.0001$.

documented by various read outs including intracellular viral double-stranded RNA and spike protein expression, as well as extracellular viral RNA. The virus was further detected by electron microscopy in cells of infected human heart slices and in an endocardial biopsy of a COVID-19 patient. Importantly, functional virus could be isolated from supernatants of infected cardiomyocytes, documenting that SARS-CoV-2 undergoes a full replicatory cycle. Of note, viral infection was confirmed with cells of two different hiPS donors and two viral strains, and our *in vitro* data are consistent with a recent online publication.[27]

The expression of the SARS-CoV-2 receptor ACE2 in cardiomyocytes was confirmed at the mRNA and protein levels, but its localization was distinct from that in Caco-2 cells. Although ACE2 could be detected at the cell membrane in some iPS-CMs, it was preferentially detected in the cytoplasm and the perinuclear region (*Figure 1D* and Supplementary material online, *Figure S1*). The preferential intracellular localization of ACE2 observed in cultured iPS-CMs was similar to the staining pattern of human heart samples,[16] and may suggest that ACE2 is shuttling between the plasma membrane and intracellular compartments. Despite the relatively low membrane ACE2 expression, ACE2 was functionally required for virus infection. Thus, recombinant ACE2 and neutralizing antibodies against ACE2 partially blocked viral spike protein expression after SARS-CoV-2 infection.

Whereas the receptor ACE2 was well expressed at the mRNA and protein level, the previously described protease activator TMPRSS2 was expressed at a very low level in hiPS-CMs, suggesting that activation of the spike protein may be mediated by other cysteine proteases such as cathepsin L and B, which also can mediate viral activation.[22] Indeed, the protease inhibitor ALLM, which preferentially blocks cathepsin L and B,[26] reduced viral spike protein expression. Viral infection was associated with cytotoxic effects and inhibition of beating of cardiomyocytes in our *in vitro* cultures and cardiospheres, suggesting a potential detrimental effect of SARS-CoV-2 infection on the human heart. Interestingly, cardiomyocytes are less susceptible to SARS-CoV-2 infection and cytotoxicity compared with $TMPRSS2^{+}$ Caco-2 cells, which showed a faster and more severe cytotoxic response. These findings, if translatable to a clinical setting, may suggest that cardiomyocyte infection may only occur under conditions of a high local virus concentration and longer time exposure. Viral infection may be facilitated in patients with cardiovascular disease, due to the described augmentation of ACE2 expression and cardiovascular disease-associated vascular inflammation allowing infiltration of virus-loaded immune cells.

SARS-CoV-2 elicits a typical transcriptional response to viral infection including the activation of interferon pathways. Since we recently demonstrated that SARS-CoV-2 infection deregulates pathways involved in endoplasmic reticulum (ER) stress and protein homeostasis,[21] one may hypothesize that viral infection may induce ER stress leading to prolonged unfolded protein response and subsequent alteration in calcium homeostasis and cardiomyocyte cell death.[28]

There is compelling evidence that patients suffering from COVID-19 show profound elevations of cardiac injury biomarkers and deteriorated right and left ventricular cardiac function; however, whether cardiac injury is directly caused by cardiomyocyte infection is unclear. Viral RNA has been detected at significant levels in cardiac tissue,[11–14] and cardiomyocyte infection may occur during conditions of vascular leakage and tissue inflammation.[29] Our data showing virus particles in cardiomyocytes of a COVID-19 patient further support that viral infection can indeed occur. However, whether a direct infection is the main cause leading to the high incidence of cardiac involvement observed after COVID-19[4] is unclear. While viral RNA meanwhile has been detected in various studies,[11–14] only few cases reported the detection of the virus particle by electron microscopy in the heart, but mainly in non-parenchymal cells.[15] It is also debated whether COVID-19 induces myocarditis. While some studies documented infiltration of inflammatory cells,[4,14] others did not find elevated inflammatory cytokines in cardiac tissue in autopsies of patients who died of COVID-19.[13] Therefore, the incidence and consequences of SARS-CoV-2 infection of cardiomyocytes in human hearts deserves further studies. Our *in vitro* data could suggest that infected cardiomyocytes may undergo apoptosis, a transient process, which may lead to secondary replacement fibrosis but not necessarily inflammation. The profound induction of interferon pathways observed in our RNA sequencing analysis may further imply an antiviral response in infected cardiomyocytes. However, these *in vitro* experiments by no means can mimic the complex effects of the virus on cellular and systemic levels. Thus, it will be important to study the presence of coronavirus particles and tissue morphology not only postmortem but also in cardiac biopsies at the first time when increased troponin release is detected, during the further progression, and after recovery in order to gain insights into a potential relationship of acute infection with cardiac injury.

Finally, the used models can serve as experimental tools for further testing the effects of therapeutic strategies. Interfering with ACE2 by neutralizing antibodies or recombinant ACE2, which was previously shown to block infection of organoids,[25] or inhibition of the RNA polymerase with remdesivir efficiently inhibited viral spike protein expression. Our findings showing that cathepsins and probably not TMPRSS2 are involved in infection of cardiomyocytes may support the testing of cathepsin L inhibitors, as recently suggested by Liu *et al.*[30]

Supplementary material

Supplementary material is available at *Cardiovascular Research* online.

Authors' contributions

D.B. designed and performed viral infection experiments, and performed statistical analysis. J.U.G.W., designed and performed cell culture and subsequent analysis, and performed statistical analysis. M.S. performed cell culture studies and subsequent analysis. G.S.A. performed cell culture studies and subsequent analysis. U.S. and A.H. provided iPS-CMs. G.L. supervised and performed histological analyses. S.G. performed and analysed the RNA sequencing study. M.D.P. and J.K. developed and provided human iPS-derived cardiospheres. P.N.H., U.H.E., and A.S.F. performed eletron microscropy studies of cell culture material. H.M. provided human heart for generation of human heart slices. A.M.Z, provided conceptual support, designed the studies, and contributed to manuscript writing. K.K. performed electron microscopy of the human case. J.C. designed and supervised virus generation and infection experiments, provided conceptual support, and contributed to manuscript writing. A.D. provided human heart slices. T.E. provided iPS-CMs and provided conceptual input for study design. C.T. provided the case report. S.C. designed and supervised all virus infection experiments and provided conceptual support. S.D. designed the experiments and wrote the draft of the manuscript. All authors have made contributions to and corrected the manuscript.

Acknowledgements

The authors thank Tatjana Starzetz [Neurological Institute (Edinger Institute), University of Frankfurt] as well as Marion Basoglu (Biological

Sciences, University of Frankfurt) for electron micrsocopy sample preparation.

Conflict of interest: none declared.

Funding

The study has been supported by the German Center for Cardiovascular Research (DZHK) and the Excellence Strategy Program of the DFG (Exc 2026). K.K. was supported by the German Heart Foundation. S.C. was supported by the Pfizer Foundation, and M.P.P. and J.K. were supported by the European Innovation Council (822455).

Data availability

The data and analytic methods will be made upon request to other researchers for purposes of reproducing the results or replicating the procedure. The study materials will only be made available if sufficient material can be provided to other researchers for purposes of reproducing the results or replicating the procedure.

References

1. Chen C, Zhou Y, Wang DW. SARS-CoV-2: a potential novel etiology of fulminant myocarditis. *Herz* 2020;**45**:230–232.
2. Huang C, Wang Y, Li X, Ren L, Zhao J, Hu Y, Zhang L, Fan G, Xu J, Gu X, Cheng Z, Yu T, Xia J, Wei Y, Wu W, Xie X, Yin W, Li H, Liu M, Xiao Y, Gao H, Guo L, Xie J, Wang G, Jiang R, Gao Z, Jin Q, Wang J, Cao B. Clinical features of patients infected with 2019 novel coronavirus in Wuhan, *China. Lancet* 2020;**395**:497–506.
3. Guzik TJ, Mohiddin SA, Dimarco A, Patel V, Savvatis K, Marelli-Berg FM, Madhur MS, Tomaszewski M, Maffia P, D'Acquisto F, Nicklin SA, Marian AJ, Nosalski R, Murray EC, Guzik B, Berry C, Touyz RM, Kreutz R, Wang DW, Bhella D, Sagliocco O, Crea F, Thomson EC, McInnes IB. COVID-19 and the cardiovascular system: implications for risk assessment, diagnosis, and treatment options. *Cardiovasc Res* 2020;**116**:1666–1687.
4. Puntmann VO, Carerj ML, Wieters I, Fahim M, Arendt C, Hoffmann J, Shchendrygina A, Escher F, Vasa-Nicotera M, Zeiher AM, Vehreschild M, Nagel E. Outcomes of cardiovascular magnetic resonance imaging in patients recently recovered from coronavirus disease 2019 (COVID-19). *JAMA Cardiol* 2020; doi:10.1001/jamacardio.2020.3557.
5. Shi S, Qin M, Shen B, Cai Y, Liu T, Yang F, Gong W, Liu X, Liang J, Zhao Q, Huang H, Yang B, Huang C. Association of cardiac injury with mortality in hospitalized patients with COVID-19 in Wuhan, China. *JAMA Cardiol* 2020;**5**:802–810.
6. Szekely Y, Lichter Y, Taieb P, Banai A, Hochstadt A, Merdler I, Gal Oz A, Rothschild E, Baruch G, Peri Y, Arbel Y, Topilsky YT. spectrum of cardiac manifestations in coronavirus disease 2019 (COVID-19)—a systematic echocardiographic study. *Circulation* 2020;**142**:342–353.
7. Arentz M, Yim E, Klaff L, Lokhandwala S, Riedo F, Chong M, Lee M. Characteristics and outcomes of 21 critically ill patients with COVID-19 in Washington State. *Jama* 2020;**323**:1612–1614.
8. To KF, Tong JHM, Chan PKS, Au FWL, Chim SSC, Chan KCA, Cheung JLK, Liu EYM, Tse GMK, Lo AWI, Lo YMD, Ng HK. Tissue and cellular tropism of the coronavirus associated with severe acute respiratory syndrome: an in-situ hybridization study of fatal cases. *J Pathol* 2004;**202**:157–163.
9. Oudit GY, Kassiri Z, Jiang C, Liu PP, Poutanen SM, Penninger JM, Butany J. SARS-coronavirus modulation of myocardial ACE2 expression and inflammation in patients with SARS. *Eur J Clin Invest* 2009;**39**:618–625.
10. Alhogbani T. Acute myocarditis associated with novel Middle east respiratory syndrome coronavirus. *Ann Saudi Med* 2016;**36**:78–80.
11. Puelles VG, Lütgehetmann M, Lindenmeyer MT, Sperhake JP, Wong MN, Allweiss L, Chilla S, Heinemann A, Wanner N, Liu S, Braun F, Lu S, Pfefferle S, Schröder AS, Edler C, Gross O, Glatzel M, Wichmann D, Wiech T, Kluge S, Pueschel K, Aepfelbacher M, Huber TB. Multiorgan and renal tropism of SARS-CoV-2. *N Engl J Med* 2020;**383**:590–592.
12. Wenzel P, Kopp S, Göbel S, Jansen T, Geyer M, Hahn F, Kreitner K-F, Escher F, Schultheiss H-P, Münzel T. Evidence of SARS-CoV-2 mRNA in endomyocardial biopsies of patients with clinically suspected myocarditis tested negative for COVID-19 in nasopharyngeal swab. *Cardiovasc Res* 2020;**116**:1661–1663.
13. Lindner D, Fitzek A, Bräuninger H, Aleshcheva G, Edler C, Meissner K, Scherschel K, Kirchhof P, Escher F, Schultheiss H-P, Blankenberg S, Püschel K, Westermann D. Association of cardiac infection with SARS-CoV-2 in confirmed COVID-19 autopsy cases. *JAMA Cardiol* 2020; doi: 10.1001/jamacardio.2020.3551.
14. Escher F, Pietsch H, Aleshcheva G, Bock T, Baumeier C, Elsaesser A, Wenzel P, Hamm C, Westenfeld R, Schultheiss M, Gross U, Morawietz L, Schultheiss H-P. Detection of viral SARS-CoV-2 genomes and histopathological changes in endomyocardial biopsies. *ESC Heart Fail* 2020; doi: 10.1002/ehf2.12805.
15. Tavazzi G, Pellegrini C, Maurelli M, Belliato M, Sciutti F, Bottazzi A, Sepe PA, Resasco T, Camporotondo R, Bruno R, Baldanti F, Paolucci S, Pelenghi S, Iotti GA, Mojoli F, Arbustini E. Myocardial localization of coronavirus in COVID-19 cardiogenic shock. *Eur J Heart Fail* 2020;**22**:911–915.
16. Nicin L, Abplanalp WT, Mellentin H, Kattih B, Tombor L, John D, Schmitto JD, Heineke J, Emrich F, Arsalan M, Holubec T, Walther T, Zeiher AM, Dimmeler S. Cell type-specific expression of the putative SARS-CoV-2 receptor ACE2 in human hearts. *Eur Heart J* 2020;**41**:1804–1806.
17. Chen L, Li X, Chen M, Feng Y, Xiong C. The ACE2 expression in human heart indicates new potential mechanism of heart injury among patients infected with SARS-CoV-2. *Cardiovasc Res* 2020;**116**:1097–1100.
18. Breckwoldt K, Letuffe-Brenière D, Mannhardt I, Schulze T, Ulmer B, Werner T, Benzin A, Klampe B, Reinsch MC, Laufer S, Shibamiya A, Prondzynski M, Mearini G, Schade D, Fuchs S, Neuber C, Krämer E, Saleem U, Schulze ML, Rodriguez ML, Eschenhagen T, Hansen A. Differentiation of cardiomyocytes and generation of human engineered heart tissue. *Nat Protoc* 2017;**12**:1177–1197.
19. Wagner JUG, Pham MD, Nicin L, Hammer M, Bottermann K, Yuan T, Sharma R, John D, Muhly-Reinholz M, Tombor L, Hardt M, Madl J, Dimmeler S, Krishnan J. Dissection of heterocellular cross-talk in vascularized cardiac tissue mimetics. *J Mol Cell Cardiol* 2020;**138**:269–282.
20. Hoehl S, Rabenau H, Berger A, Kortenbusch M, Cinatl J, Bojkova D, Behrens P, Böddinghaus B, Götsch U, Naujoks F, Neumann P, Schork J, Tiarks-Jungk P, Walczok A, Eickmann M, Vehreschild MJGT, Kann G, Wolf T, Gottschalk R, Ciesek S. Evidence of SARS-CoV-2 infection in returning travelers from Wuhan, China. *N Engl J Med* 2020;**382**:1278–1280.
21. Bojkova D, Klann K, Koch B, Widera M, Krause D, Ciesek S, Cinatl J, Münch C. SARS-CoV-2 infected host cell proteomics reveal potential therapy targets. *Nature* 2020;**583**:469–472.
22. Hoffmann M, Kleine-Weber H, Schroeder S, Krüger N, Herrler T, Erichsen S, Schiergens TS, Herrler G, Wu N-H, Nitsche A, Müller MA, Drosten C, Pöhlmann S. SARS-CoV-2 cell entry depends on ACE2 and TMPRSS2 and is blocked by a clinically proven protease inhibitor. *Cell* 2020;**181**:271–280.
23. Cinatl J, Morgenstern B, Bauer G, Chandra P, Rabenau H, Doerr HW. Treatment of SARS with human interferons. *Lancet* 2003;**362**:293–294.
24. Fischer C, Milting H, Fein E, Reiser E, Lu K, Seidel T, Schinner C, Schwarzmayr T, Schramm R, Tomasi R, Husse B, Cao-Ehlker X, Pohl U, Dendorfer A. Long-term functional and structural preservation of precision-cut human myocardium under continuous electromechanical stimulation *in vitro*. *Nat Commun* 2019;**10**:117.
25. Monteil V, Kwon H, Prado P, Hagelkrüys A, Wimmer RA, Stahl M, Leopoldi A, Garreta E, Hurtado Del Pozo C, Prosper F, Romero JP, Wirnsberger G, Zhang H, Slutsky AS, Conder R, Montserrat N, Mirazimi A, Penninger JM. Inhibition of SARS-CoV-2 infections in engineered human tissues using clinical-grade soluble human ACE2. *Cell* 2020;**181**:905–913.
26. Sasaki T, Kishi M, Saito M, Tanaka T, Higuchi N, Kominami E, Katunuma N, Murachi T. Inhibitory effect of di- and tripeptidyl aldehydes on calpains and cathepsins. *J Enzyme Inhib* 1990;**3**:195–201.
27. Sharmam A, Garcia G, Arumugaswami V, Svendsen CN. Human iPSC-derived cardiomyocytes are susceptible to SARS-CoV-2 infection. *BioRxiv* 2020;**04.21.0519**.
28. Kitakaze M, Tsukamoto O. What is the role of ER stress in the heart? Introduction and series overview. *Circ Res* 2010;**107**:15–18.
29. Varga Z, Flammer AJ, Steiger P, Haberecker M, Andermatt R, Zinkernagel AS, Mehra MR, Schuepbach RA, Ruschitzka F, Moch H. Endothelial cell infection and endotheliitis in COVID-19. *Lancet* 2020;**395**:1417–1418.
30. Liu T, Luo S, Libby P, Shi G-P. Cathepsin L-selective inhibitors: a potentially promising treatment for COVID-19 patients. *Pharmacol Ther* 2020;**213**:107587.

Translational perspective

Although this study cannot address whether cardiac injury and dysfunction in COVID-19 patients is caused by direct infection of cardiomyocytes, the demonstration of direct cardiotoxicity in cardiomyocytes, organ mimics, human heart slices, and human hearts warrants the further monitoring of cardiotoxic effects in COVID-19 patients.

SUPPLEMENTAL MATERIAL

Supplemental Methods **Page 1**

Supplemental Figures **Page 8**

Supplemental Methods

Cells and cardiac tissues

Human induced pluripotent stem cell-derived cardiomyocytes (hiPS-CM) were generated of two donors (two batches for each donor) with an embryoid body based protocol as previously described[1] and were frozen at day 15-17. Thawed cardiomyocytes were seeded at a density of 4.2×10^6 cells/24-well plate coated with 0.1 % gelatine. hiPS-CM were cultured in RPMI/B27 medium at 37 °C, 5 % CO_2 4 to 5 days prior to viral infection. Medium was changed every second day. Purity of iPS-CM was tested by FACS analysis of troponin T and was 93±4% for the four batches. All procedures involving the generation of hiPSC lines and cardiac differentiation were approved by the local ethics committee in Hamburg (Az PV4798, 28.10.2014). Cardiospheres were generated by adapting a previously described protocol[2] using commercially available hiPS cells. Briefly, the hiPS line WSTIi081-A (EBiSC) was cultured in TeSRTM-E8TM iPSCs medium (Stemcell) at 37 °C and 5 % CO_2 to a confluence of 90-95%. hiPSCs were differentiated to hiPS-derived cardiomyocytes (hiPS-CMs) with STEMdiff™ Cardiomyocyte Differentiation Kit (Stemcell) following manufacturer instructions. At day 17, contracting hiPS-CMs were harvested with STEMdiff™ Cardiomyocyte Dissociation Kit (Stemcell) and aggregated to form cardiospheres in AggreWellTM800 microwell culture plates (Stemcell) at a density of 4000 hiPS-CMs per microwell. hiPSC-CMs were cultured for 48 hours in STEMdiff™ Support medium (Stemcell) to form cardiac spheroids. Cardiospheres were then transferred to single well in ultra-low-attachment 96-well plate (Corning) and cultured in STEMdiff™ Cardiomyocyte Maintenance medium (Stemcell) for 4 days prior to infection.

Living human heart slices were generated and cultured as recently described[9]. Samples of left ventricular myocardium were taken from failing hearts at the time of transplantation by the Clinic of Thoracic and Cardiovascular Surgery, Heart and Diabetes Center, Bad Oeynhausen, Germany. The procedure has been approved by the institutional ethics board, and patients have provided informed consent to the scientific use of the explanted tissue. In brief, heart slices were generated from explanted failing human myocardium by cutting 300 µm thick sections with a vibratome. Slices were mounted and cultured in biomimetic culture chambers that were operated on a continuously agitated platform in a standard incubator (37 °C, 5% CO_2, 20% O_2, 80% humidity)[3]. Pacing was performed at 0.5 Hz with bipolar 50 mA pulses comprised of 1 ms charging and discharging pulses separated by a 1 ms interval. Slices were cultured in Medium 199 supplemented with penicillin/streptomycin, insulin/transferrin/selenite and 50 µM 2-mercaptoethanol. Medium was exchanged in part (1.6 ml of 2.4 ml total volume in each BMCC) at 36–48 h intervals.

Patient characteristic

The patient (27 years, male) was diagnosed with COVID-19 by PCR of nasal swabs and was suffering from compromised cardiac function (EF: 44 %). After exclusion of coronary heart disease, endomyocardial biopsies (EMB) were taken following a standard protocol[4]. The patient provided written consent for the procedures *(ethic vote number: EA2/140/16).* Lymphocytic myocarditis was diagnosed by the presence of abnormal inflammatory infiltrate within the myocardium: ≥14 leucocytes/mm2 including up to 4 monocytes/mm2 and ≥7 cells/mm of CD 3 positive T-lymphocytes.

Infection

SARS-CoV-2-FFM1 and FFM2 were isolated and propagated in Caco-2 cells as previously described [5,6]. For infection of hiPS-CMs, the viral stock was diluted to desired MOI in the respective medium and incubated with cells for 2 h. Then the infectious inoculum was removed and cells were supplemented the respective hiPSC-CM culture media (see above). Cardiospheres were cultured with 25µl of viral stock (1.10^7 TCID50/ml) for three to five days in STEMdiff™ Cardiomyocyte Maintenance medium (Stemcell). EHTs were incubated with 200µl of viral stock (1.10^7 TCID50/ml) for three to five days in the presence of 2 % horse serum. Living human heart slices were incubated with 200µl of viral stock (1.10^7 TCID50/ml) for three to five days using the above mentioned medium without mercaptoethanol.

For experiments addressing receptor utilization, cells were pretreated with 80 µg/mL anti-human ACE2 antibody 30 minutes prior to infection (R&D Systems, goat, AF933). As antibody isotype control an unrelated anti-mCherry antibody (SICGEN, goat, AB0081-20) in concentration 80 µg/mL was used. Recombinant human ACE2 protein (R&D Systems, 933-ZN) in concentration 5µg/ml was mixed with virus and incubated 30 minutes prior to infection. In order to inhibit cathepsins B/L, 1 µM of N-Acetyl-L-leucyl-L-leucyl-L-methional (Tocris, 0384) diluted in DMSO was added during and post infection. For experiments involving viral RNA-dependent RNA polymerase inhibitor remdesivir (synthesized at Johnson & Johnson, 1 µM) cells were treated with the respective chemical only post infection.

RT-qPCR

Quantification of SARS-CoV RNA in cell culture supernatants was performed as previously described [6]. Briefly, RNA from supernatants was isolated using AVL buffer and the QIAamp Viral RNA Kit (Qiagen) according to the manufacturer's instructions. RNA was subjected to OneStep qRT-PCR analysis using the SYBR green based Luna Universal One-Step RT154 qPCR Kit (New England Biolabs) and a CFX96 Real-Time System, C1000 Touch Thermal Cycler.

qPCR and gel electrophoresis

Total RNA from hiPSC, hiPS-CMs, hiPS-derived cardiospheres and CaCo-2 was isolated using RNeasy Micro Kit (Qiagen) according manufacturer's instructions. Reverse transcription was performed using 1000 ng RNA, random hexamers and MuLV reverse transcriptase (Thermo Fisher). Fast SYBR Green qPCR were carried out by StepOnePlus real-time PCR systems (Thermo Fisher). RPLP0 amplification was used as house-keeping gene for data normalization. Relative expression levels were calculated by $2^{-\Delta Ct}$.

Quantification of ACE2 and TMPRSS2 was performed with the following primers:
hRPLP0-F: 5'-TCGACAATGGCAGCATCTAC-3'
hRPLP0-R: 5'-ATCCGTCTCCACAGACAAGG-3'
ACE2-F: 5'-CATTGGAGCAAGTGTTGGATCTT-3'
ACE2-R: 5'-GAGCTAATGCATGCCATTCTCA-3'
TMPRSS2-F: 5'-CTGCCAAGGTGCTTCTCATT-3'
TMPRSS2-R: 5'-CTGTCACCCTGGCAAGAATC-3'

Amplified samples were run on 1% agarose gel in 1xTAE buffer (120 V) and visualized with Midori Green Advance (see Suppl. Fig. 5).

Quantification of virus titer in cell culture supernatants

Supernatants from infected hiPS-CMs were collected 48h post infection. Confluent layers of CaCo-2 cells in 96-well plates were infected with serially diluted supernatants. Cytopathogenic effect (CPE) was assessed visually 48 h after infection. The infectious titer was determined as TCID50/ml.

Immunostaining of viral dsRNA and spike protein

hiPS-CMs were fixed with ice cold acetone/methanol (60:40) for 10 minutes at RT. Immunostaining was performed using a monoclonal antibody directed against dsRNA (1:150 dilution, SCICONS J2, mouse, IgG2a, kappa chain, English & Scientific Consulting Kft., Szirák, Hungary) and rabbit anti-Spike (1:1500, Sino Biological) followed by peroxidase conjugated anti-rabbit secondary antibody (1:1000, Dianova). The dsRNA was detected with biotin-conjugated secondary antibody (1:1000 dilution, Jackson ImmunoResearch) followed by application of streptavidin, peroxidase conjugate (1:3000 dilution, Sigma Aldrich). Both the dsRNA and spike protein positive cells were visualized by addition of AEC substrate. Images were analyzed using NIH ImageJ.

Immunofluorescence Labeling

hiPS-CM were fixed with ice cold acetone/methanol (60:40) or 4% PFA and were permeabilized with 0.1 % Triton X-100. Prior to primary antibody labeling, cells were blocked with 5% donkey serum in PBS or 1% BSA and 2% goat serum in PBS for 60 minutes at RT.

Human cardiospheres were stained as described[2]. In brief, cardiospheres were fixed with 4 % HistoFix (Carl Roth GmbH) for 60 minutes and then were permeabilized with 0.2 % Triton X-100 in PBS (PBSTT) for additional 60 minutes. Cardiospheres were blocked with 5 % goat serum in 1 % Tween / 0.002 % Triton X-100 in PBS for 30 minutes before adding primary antibodies.

Heart slices were fixed in 4 % HistoFix (Carl Roth GmbH) for 24 h at 4°C. Slices were transferred to an ascending sucrose series of 4 % sucrose in PBS (1 h, 4°C), 15 % sucrose in PBS (4 h, 4°C) and 30 % sucrose in PBS (overnight, 4°C) and were washed twice in 100 mM glycine (each 30 minutes, at 4°C). After incubating in PBS for 30 minutes, at 4°C, slices were permeabilized with 1 % Triton X-100 in PBS (overnight, at 4°C). Slices were washed thrice with PBS (each 30 minutes, at 4°C) and blocked with 3% BSA in 0.3 % Triton X-100 (overnight, at 4°C). Slices were again washed trice in 0.1 % Triton X-100 and incubated with primary antibodies.

The following antibodies were used:

Primary antibodies:

Antibody	Product code
Monoclonal Anti-α-Actinin (Sarcomeric) antibody produced in mouse (1:300)	A7811, Sigma-Aldrich
Monoclonal anti-cardiac Actin antibody produced in mouse (1:300)	61075, Progen
Polyclonal Human ACE-2 Antibody produced in goat (1:100)	AF933, R&D Systems.

Polyclonal Human ACE-2 Antibody produced in rabbit (1:100)	ab15348, Abcam
Monoclonal SARS-CoV-2 (2019-nCoV) Spike S1 Antibody, produced in rabbit (1:1500 / 1:100)	40150-R007, Sino Biological
Monoclonal Cleaved Caspase-3 (Asp175) (5A1E), produced in rabbit (1:100)	9664, Cell Signaling Technology
Monoclonal antibody directed against dsRNA, produced in mouse (1:150)	10010500, SCICONS J2, English & Scientific Consulting Kft., Szirák, Hungary
Polyclonal anti-mCherry antibody, produced in goat	AB0081-20, SICGEN

Secondary antibodies:

Antibody	Product code
Donkey anti-Rabbit IgG (H+L) Highly Cross-Adsorbed Secondary Antibody, Alexa Fluor 488 (1:200)	A-21206, Invitrogen
Donkey anti-Mouse IgG (H+L) Highly Cross-Adsorbed Secondary Antibody, Alexa Fluor Plus 647 (1:200)	A32787, Invitrogen
Donkey anti-Goat IgG (H+L) Cross-Adsorbed Secondary Antibody, Alexa Fluor 555 (1:200)	A-21432, Invitrogen
Goat anti-Rabbit IgG (H+L), Superclonal™ Recombinant Secondary Antibody, Alexa Fluor 555 (1:200)	A27039 , Invitrogen
Goat anti-Mouse IgG (H+L) Highly Cross-Adsorbed Secondary Antibody, Alexa Fluor Plus 488 (1:200)	A32723, Invitrogen
Goat anti-Rabbit IgG (H+L) Peroxidase AffiniPure (1:1000)	111-035-144, Jackson ImmunoResearch
Goat Anti-Rabbit IgG (H+L) Biotin-SP (long spacer) AffiniPure $F(ab')_2$ Fragment (1:1000)	111-066-003, Jackson ImmunoResearch

In addition:

Alexa Fluor™ 647 Phalloidin (1:100)	A22287, Invitrogen
Ulex Europaeus Agglutinin I (UEA I), Biotinylated (1:50)	B-1065-2, Vector Laboratories
DAPI (1:1000)	62248, Thermo Scientific™
Streptavidin, Peroxidase Conjugate (1:3000)	189733 Sigma-Aldrich

hiPS-CM and heart slices were mounted with Fluoromount-G (Invitrogen). Cardiospheres were mounted with ProLong Gold Antifade (Invitrogen - P3693-4). hiPS-CM images were taken using an inverted fluorescence microscope (Nikon Eclipse Ti2 fluorescence microscope) and Leica SP8 confocal inverted microscope. Cardiac slices images were taken using a Leica SP8 confocal inverted microscope and quantified using Volocity software version 6.5 (Quorum Technologies).

Electron microscopy

Human heart slices: For ultrastructural analysis human heart slices were fixed for 24h in 3% phosphate buffered paraformaldehyde. Samples were postfixed in 1% osmium tetroxide in the same buffer for 1 h and stained en bloc in 1% uranyl acetate in 10% ethanol for 1 h, dehydrated in ethanol, and embedded in epon. Semithin sections were stained with toluidine blue. Thin sections (50 nm nominal thickness) were stained with methanolic uranyl acetate and Reynold's lead citrate and examined in a Tecnai F30 Transmission Electron Microscope (Thermo Fisher Scientific, Waltham, MA, U.S.A.) equipped with a US4000 CCD camera (Gatan, Pleasanton, CA, U.S.A.). Regions of interest were located using SerialEM software[7] in montages done at x2,300 magnification, high magnification montaged images were recorded at x9,400 and x23,000 (1.3 and 0.49 nm pixel size, respectively).

Patient biopsy: For electron microscopy, tissues were fixed in 2.5% glutaraldehyde (Paesel-Lorei, Frankfurt, Germany) buffered in 0.1 M cacodylate buffer (pH 7.4). Then, tissues were postfixed in 1% OsO_4 in 0.1 M cacodylate buffer and then dehydrated in an ethanol series (50, 70, 96, 100%). The 70% ethanol was saturated with uranyl acetate for contrast enhancement. The specimens were embedded in Araldite (Serva, Heidelberg, Germany). Semi- and ultra-thin sections were taken on a FCR Reichert Ultracut ultramicrotome (Leica, Bensheim, Germany). Ultrathin sections were contrasted with lead citrate and analyzed and documented with an EM10A electron microscope (Carl Zeiss, Oberkochen, Germany).

RNA sequencing

hiPS-CM were lysed with RLT buffer after 48h post infection and total RNA was isolated using RNeasy Mini Kit (Qiagen) according manufacturer's instructions. RNA and library preparation integrity were verified with LabChip Gx Touch 24 (Perkin Elmer). 250ng of total RNA was used as input for Truseq Stranded Total RNA Library preparation following the low sample protocol (Illumina). Sequencing was performed on the NextSeq500 instrument (Illumina) using v2 chemistry, resulting in average of 50M reads per library with 1x75bp single end setup. The resulting raw reads were assessed for quality, adapter content and duplication rates with FastQC[8]. Trimmomatic version 0.39 was employed to trim reads after a quality drop below a mean of Q20 in a window of 5 nucleotides[9]. Only reads between 30 and 150 nucleotides were cleared for further analyses. Trimmed and filtered reads were aligned versus the Ensembl human genome version hg38 (GRCh38) using STAR 2.6.1d with the parameter "--outFilterMismatchNoverLmax 0.1" to increase the maximum ratio of mismatches to mapped length to 10%[10]. The number of reads aligning to genes was counted with featureCounts 1.6.5 tool from the Subread package[11]. Only reads mapping at least partially inside exons were admitted and aggregated per gene. Reads overlapping multiple genes or aligning to multiple regions were excluded. Differentially expressed genes were identified using DESeq2 version 1.26.0 (Love et al., Moderated estimation of fold change and dispersion for RNA-Seq data with DESeq2). Only genes with a minimum fold change of +- 2 (log2 = +-1), a maximum Benjamini-

Hochberg corrected p-value of 0.05, and a minimum combined mean of 5 reads were deemed to be significantly differentially expressed. The Ensemble annotation was enriched with UniProt data (release 17.12.2018) based on Ensembl gene identifiers (Activities at the Universal Protein Resource (UniProt)). The data are shown in Supplemental Data file.

Statistical analysis

Data are biological replicates and are represented as mean and error bars indicating standard error of the mean (SEM). Data were statistically assessed for Gaussian distribution using Shapiro-Wilk, Kolmogorov-Smirnov and Anderson-Darling test. For comparison of two groups, statistical power was determined using two-sided, unpaired t-test. For multiple comparisons, ordinary one-way ANOVA with a post hoc Tukey's, Holm-Sidak's or Dunett's multiple comparison (parametric data) or a Kruskal-Wallis test with a post hoc Dunn's multiple comparison (non-parametric) was used.

References

1. Breckwoldt, K. *et al.* Differentiation of cardiomyocytes and generation of human engineered heart tissue. *Nat. Protoc.* **12**, 1177–1197 (2017).
2. Wagner, J. U. G. *et al.* Dissection of heterocellular cross-talk in vascularized cardiac tissue mimetics. *J. Mol. Cell. Cardiol.* **138**, 269–282 (2020).
3. Fischer, C. *et al.* Long-term functional and structural preservation of precision-cut human myocardium under continuous electromechanical stimulation in vitro. *Nat. Commun.* **10**, 117 (2019).
4. Tschöpe, C., Kherad, B. & Schultheiss, H.-P. How to perform an endomyocardial biopsy? *Turk Kardiyol. Dern. Ars.* **43**, 572–575 (2015).
5. Hoehl, S. *et al.* Evidence of SARS-CoV-2 Infection in Returning Travelers from Wuhan, China. *The New England journal of medicine* vol. 382 1278–1280 (2020).
6. Bojkova, D. *et al.* SARS-CoV-2 infected host cell proteomics reveal potential therapy targets. *Nature* **doi: 10.10**, (2020).
7. Mastronarde, D. N. Automated electron microscope tomography using robust prediction of specimen movements. *J. Struct. Biol.* **152**, 36–51 (2005).
8. Wingett, S. W. & Andrews, S. FastQ Screen: A tool for multi-genome mapping and quality control. *F1000Research* **7**, 1338 (2018).
9. Bolger, A. M., Lohse, M. & Usadel, B. Trimmomatic: a flexible trimmer for Illumina sequence data. *Bioinformatics* **30**, 2114–2120 (2014).
10. Dobin, A. *et al.* STAR: ultrafast universal RNA-seq aligner. *Bioinformatics* **29**, 15–21 (2013).
11. Liao, Y., Smyth, G. K. & Shi, W. featureCounts: an efficient general purpose program for assigning sequence reads to genomic features. *Bioinformatics* **30**, 923–930 (2014).

Supplemental Figures for the Manuscript:

SARS-CoV-2 infects and induces cytotoxic effects in human cardiomyocytes

Supplemental Figure 1

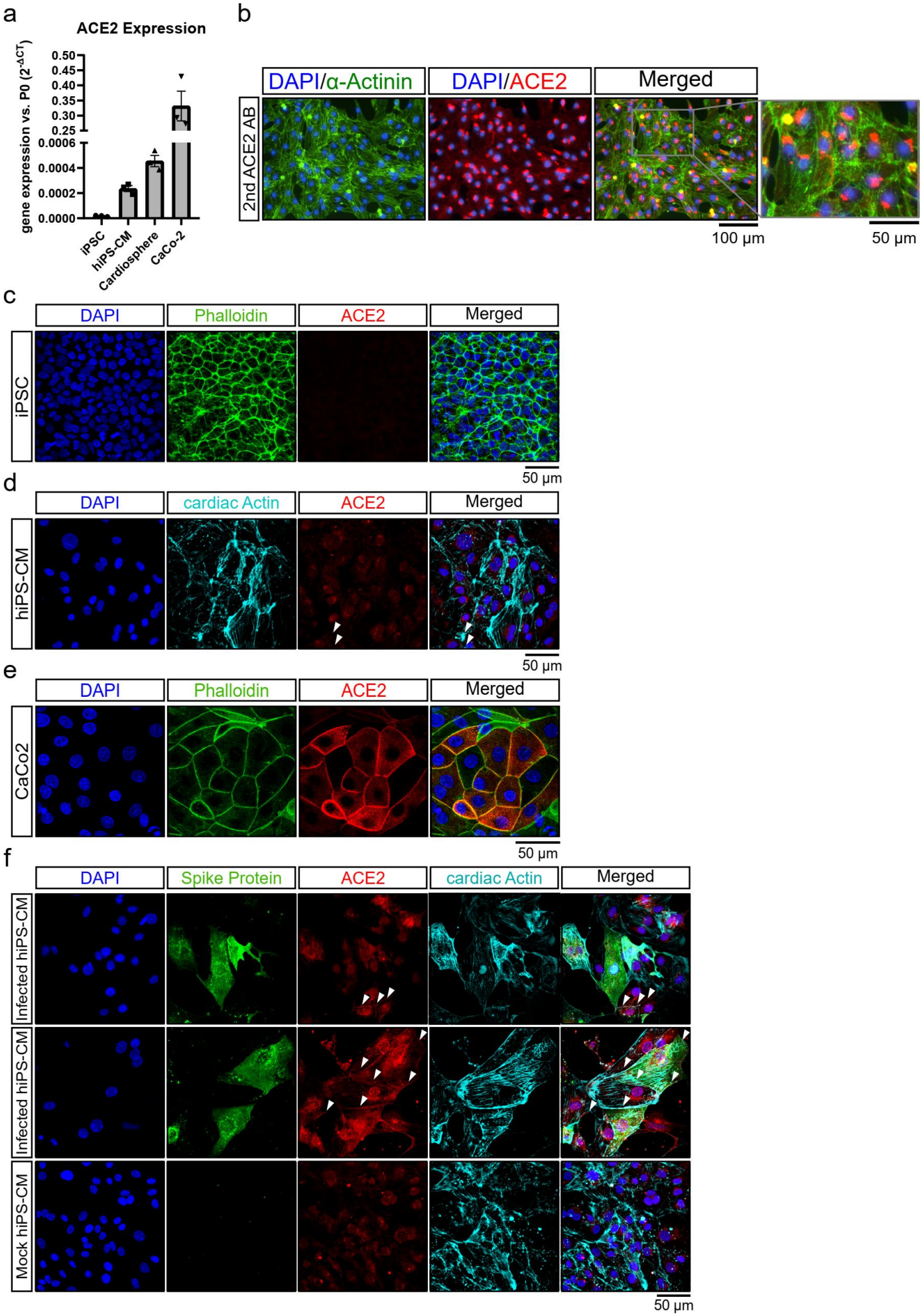

Supplemental Figure 1: ACE2 expression in control cells. (a) ACE2 expression was detected on RNA level in human iPS cells (iPSC), hiPS-cardiomyocytes, cardiospheres and colon carcinoma cells (CaCo-2). Human ribosomal RNA P0 served as housekeeping control. (b) ACE2 (red) expression was detected in hiPS-CM using another anti-ACE2 antibody (Abcam; ab15348). DAPI (blue) and α-Actinin (green) served as counterstain. (c-e) ACE2 expression (red) on protein level in iPS-cells (iPSC, c), hiPS-CM (d) and CaCo-2 cells (e). Membranous ACE2 localization is indicated by white arrows. DAPI (blue) and phalloidin (green) or cardiac actin (cyano) served as counterstain. (f) Spike protein (green) and ACE2 (red) expression in infected vs. mock hiPS-CMs. Membranous ACE2 localization is indicated by white arrows. DAPI (blue) and cardiac actin (cyano) serve as counterstain. A representative experiment is shown for each panel.

Supplemental Figure 2

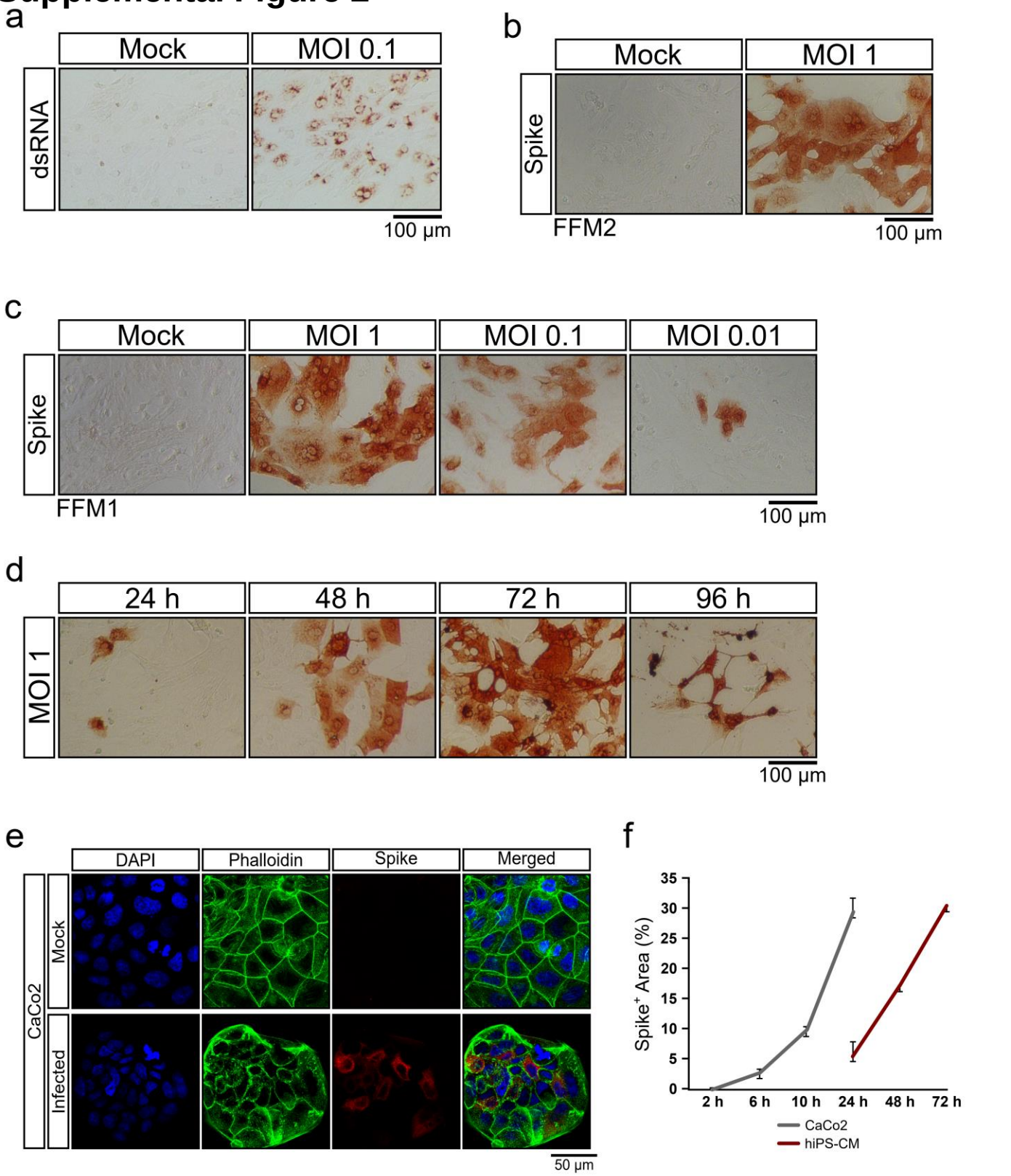

Supplemental Figure 2: dsRNA and Spike Protein detection after infection. (a) Immunostaining of double-stranded RNA (dsRNA) in hiPS-CMs after infection with SARS-CoV-2 FFM1 for 48 h. (b-d) Spike glyocoprotein was measured by immunohistochemistry after infection with isolate SARS-CoV-2 FFM2 (b) or SARS-CoV-2 FFM1 (c, d). (e) Human colon carcinoma cells (CaCo2) 24h after mock vs. SARS-CoV-2 (MOI 1) infection and stained for Spike (red), phalloidin (green) and DAPI (blue). n=3. (f) Time course experiment of infected hiPS-CM and CaCo2 cells. CaCo-2 cells (grey) and hiPS-CM were infected with SARS-CoV-2. Spike protein expression was observed by immunohistochemistry in CaCo-2 cells after 2h, 6h, 10h and 24h and in hiPS-CM after 24h, 48h and 72h. Data are shown as mean +/- SEM. n=3.

Supplemental Figure 3

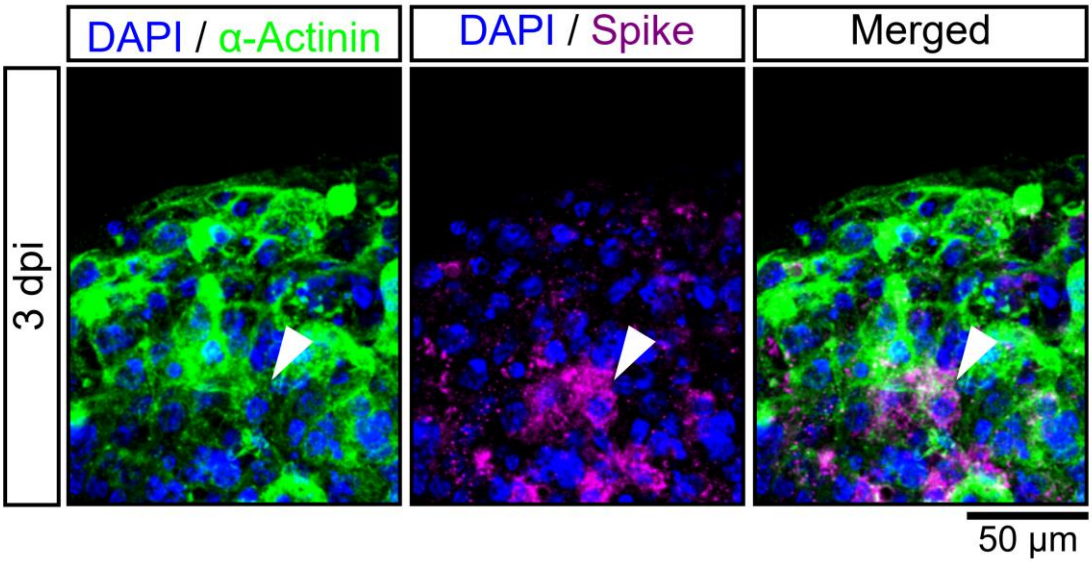

Supplemental Figure 3: Spike Protein expression in infected cardiospheres. Shown is a single z-plane of a representative cardiosphere after 3 days of SARS-CoV2 infection (3 dpi). Spike Protein (magenta) can be found perinuclear and cytoplasmatic in distinct cardiomyocytes, indicated representatively by white arrow. DAPI (blue) and α-Actinin (green) serve as counterstaining.

Supplemental Figure 4

a

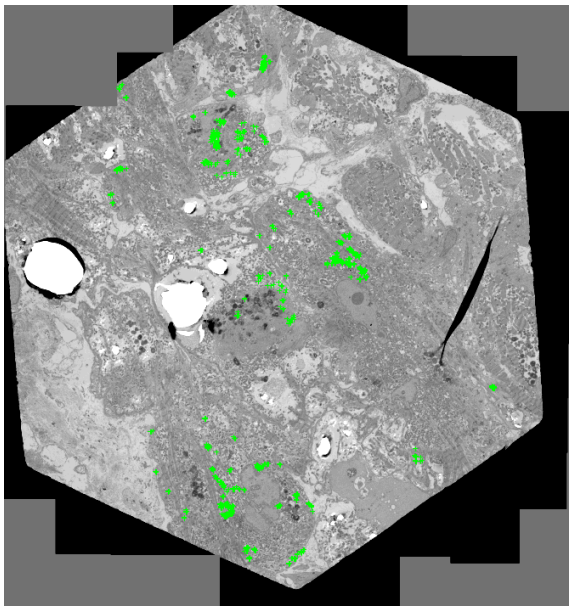

b

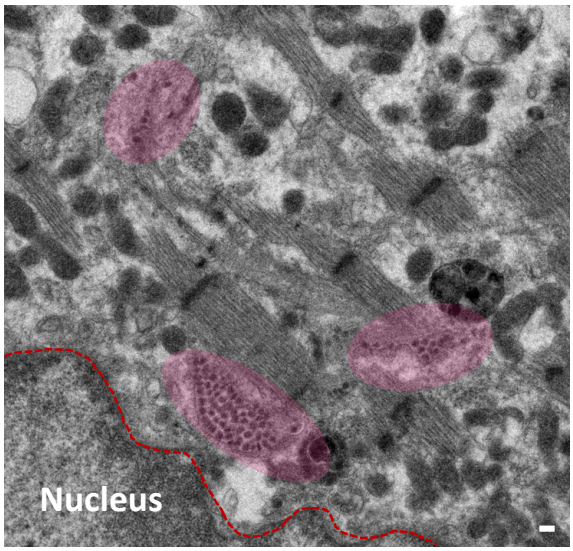

c

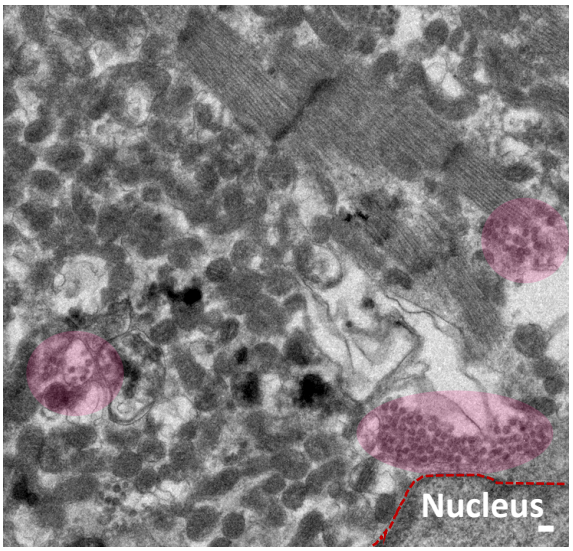

Supplemental Figure 4: Viral particles in infected heat slices. (a) Overview image of a grid square of a infected human heart slice. Infected areas are indiated by green crosses. (b, c) Transelectron microscopy images of heart slices after SARS-CoV-2 infection. Cluster of viral particles (highlighted in rose) can be found close to actinin fibres and the nucleus (red lines). Scale = 200 nm.

Supplemental Figure 5

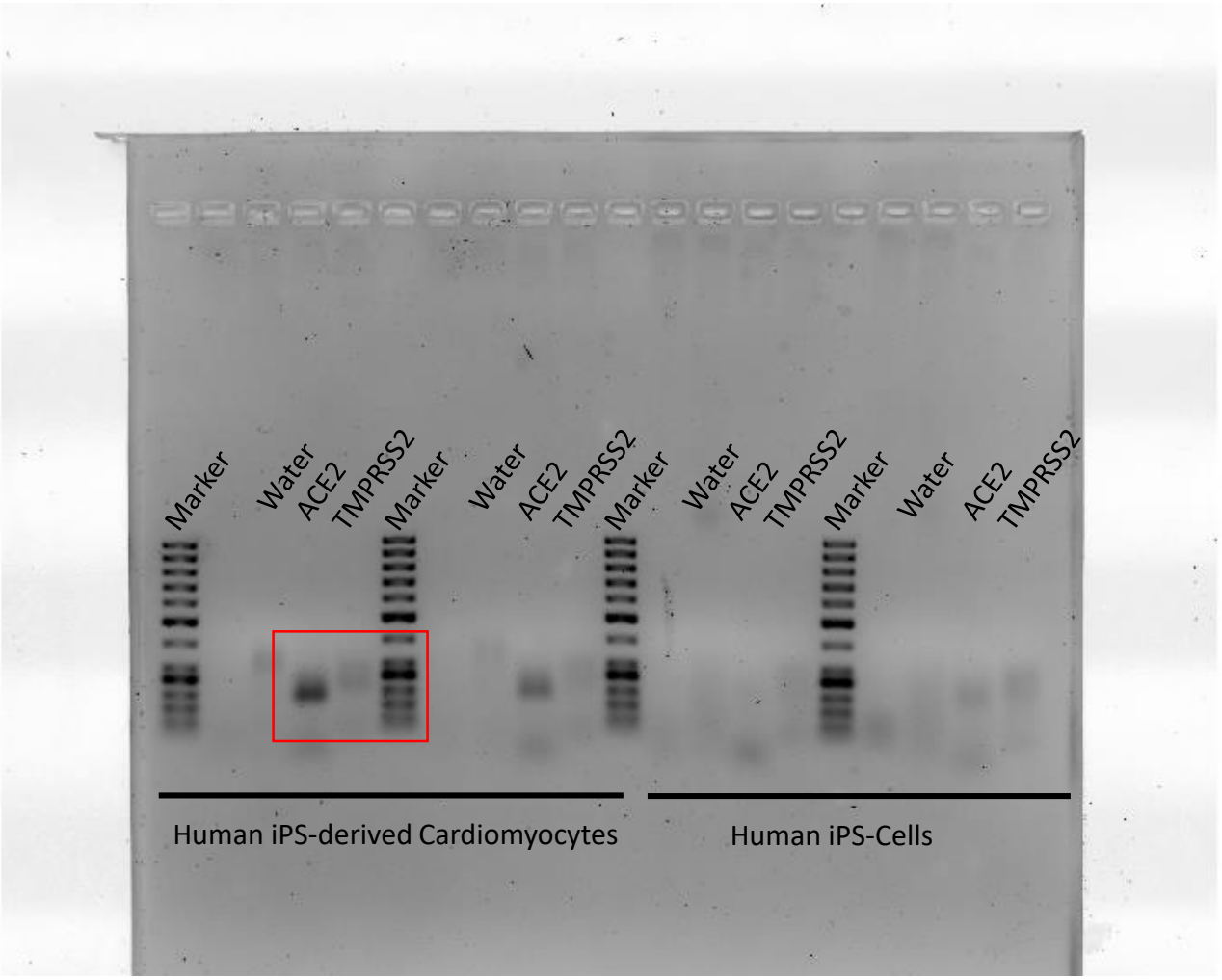

Supplemental Figure 5: Agarose gel electrophoresis of PCR products. Shown are PCR products of ACE2, TMPRSS2 and the water control in two different samples of human iPS-derived cardiomyocytes and undifferentiated human iPS-cells. Red square indicates insert used for main figure 1.